Ultra-low power fiber-coupled gallium arsenide photonic crystal cavity electro-optic modulator

Gary Shambat,[1,*] Bryan Ellis,[1] Marie A. Mayer,[2] Arka Majumdar,[1] Eugene E. Haller,[2] and Jelena Vučković[1]

[1]*Department of Electrical Engineering, Stanford University, Stanford, California 94305, USA*
[2]*Materials Sciences Division, Lawrence Berkeley National Laboratory, Berkeley, California 94720, USA, and Department of Materials Science, University of California, Berkeley, Berkeley, California 94720, USA*
*gshambat@stanford.edu

Abstract: We demonstrate a gallium arsenide photonic crystal cavity injection-based electro-optic modulator coupled to a fiber taper waveguide. The fiber taper serves as a convenient and tunable waveguide for cavity coupling with minimal loss. Localized electrical injection of carriers into the cavity region via a laterally doped *p-i-n* diode combined with the small mode volume of the cavity enable ultra-low energy modulation at sub-fJ/bit levels. Speeds of up to 1 GHz are demonstrated with photoluminescence lifetime measurements revealing that the ultimate limit goes well into the tens of GHz.

© 2011 Optical Society of America

OCIS codes: (230.3120) Integrated optics devices; (350.4238) Nanophotonics and photonic crystals; (250.4110) Modulators; (230.5750) Resonators.

References and links

1. W. M. Green, M. J. Rooks, L. Sekaric, and Y. A. Vlasov, "Ultra-compact, low RF power, 10 Gb/s silicon Mach-Zehnder modulator," Opt. Express **15**(25), 17106–17113 (2007).
2. Q. Xu, B. Schmidt, S. Pradhan, and M. Lipson, "Micrometre-scale silicon electro-optic modulator," Nature **435**(7040), 325–327 (2005).
3. T. Tanabe, K. Nishiguchi, E. Kuramochi, and M. Notomi, "Low power and fast electro-optic silicon modulator with lateral p-i-n embedded photonic crystal nanocavity," Opt. Express **17**(25), 22505–22513 (2009).
4. P. Dong, S. Liao, D. Feng, H. Liang, D. Zheng, R. Shafiiha, C.-C. Kung, W. Qian, G. Li, X. Zheng, A. V. Krishnamoorthy, and M. Asghari, "Low V$_{pp}$, ultralow-energy, compact, high-speed silicon electro-optic modulator," Opt. Express **17**(25), 22484–22490 (2009).
5. D. A. B. Miller, "Device requirements for optical interconnects to silicon chips," Proc. IEEE **97**(7), 1166–1185 (2009).
6. B. R. Bennett, R. A. Soref, and J. A. Del Alamo, "Carrier-induced change in refractive index of InP, GaAs, and InGaAsP," IEEE J. Quantum Electron. **26**(1), 113–122 (1990).
7. K. Nozaki, T. Tanabe, A. Shinya, S. Matsuo, T. Sato, H. Taniyama, and M. Notomi, "Sub-femtojoule all-optical switching using a photonic-crystal nanocavity," Nat. Photonics **4**(7), 477–483 (2010).
8. D. Englund, B. Ellis, E. Edwards, T. Sarmiento, J. S. Harris, D. A. B. Miller, and J. Vuckovic, "Electrically controlled modulation in a photonic crystal nanocavity," Opt. Express **17**(18), 15409–15419 (2009).
9. Y. Akahane, T. Asano, B. S. Song, and S. Noda, "High-Q photonic nanocavity in a two-dimensional photonic crystal," Nature **425**(6961), 944–947 (2003).
10. B. Ellis, T. Sarmiento, M. Mayer, B. Zhang, J. Harris, E. E. Haller, and J. Vuckovic, "Electrically pumped photonic crystal nanocavity light sources using a laterally doped p-i-n junction," Appl. Phys. Lett. **96**(18), 181103 (2010).
11. G. Shambat, Y. Gong, J. Lu, S. Yerci, R. Li, L. Dal Negro, and J. Vučković, "Coupled fiber taper extraction of 1.53 microm photoluminescence from erbium doped silicon nitride photonic crystal cavities," Opt. Express **18**(6), 5964–5973 (2010).
12. G. Shambat, K. Rivoire, J. Lu, F. Hatami, and J. Vučković, "Tunable-wavelength second harmonic generation from GaP photonic crystal cavities coupled to fiber tapers," Opt. Express **18**(12), 12176–12184 (2010).
13. B. Ellis, M. Mayer, G. Shambat, T. Sarmiento, J. Harris, E. E. Haller, and J. Vuckovic, "Ultra-low threshold, electrically pumped quantum dot photonic crystal nanocavity laser," to be published in Nat. Photonics (2011).
14. T. Tanabe, H. Sumikura, H. Taniyama, A. Shinya, and M. Notomi, "All-silicon sub-Gb/s telecom detector with low dark current and high quantum efficiency on chip," Appl. Phys. Lett. **96**(10), 101103 (2010).
15. D. Englund, H. Altug, and J. Vuckovic, "Low-threshold surface-passivated photonic crystal nanocavity laser," Appl. Phys. Lett. **91**(7), 071124 (2007).
16. S. Manipatruni, K. Preston, L. Chen, and M. Lipson, "Ultra-low voltage, ultra-small mode volume silicon microring modulator," Opt. Express **18**(17), 18235–18242 (2010).

1. Introduction

The success of future optical interconnects relies heavily on the performance capabilities of compact electro-optic modulators, designed to transfer an electronic bit stream onto an optical carrier wave. Tremendous progress has been made in this field over the last decade, with initial large and power hungry Mach-Zehnder based modulators being replaced by compact and efficient cavity-based designs [1–3]. Contemporary microring modulators, for example, are capable of 10's of GHz speed at energies as low as 50 fJ/bit [4]. Fueling this continued miniaturization and strive for low power is the overshadowing constraint that complete optical interconnect links should aim for ~fJ/bit targets in order to effectively compete with standard electronic connections [5].

Typical modulators are fabricated on a silicon on insulator (SOI) platform, so chosen to match the CMOS standard of integrated circuits. While this is a natural approach, the ambiguity of whether optical sources will originate on- or off-chip in a silicon-based or III-V material is still a topic of debate; thus the possibility of combining a III-V modulator with a III-V laser source could be a superior alternative. Gallium arsenide (GaAs) has a stronger free carrier dispersion coefficient than silicon by a factor of six and has fast carrier recombination at etched hole boundaries [6,7]. In our previous study, we used a vertical *p-i-n* structure in GaAs to show modulation inside a photonic crystal (PC) cavity [8]. However, this structure suffered from inefficient electrical injection into the active area as well as large heating effects due to the high currents needed for operation. Carrier spreading within thin doped PC membranes is poor and the majority of the electrical current traveled directly between the contacts. Here we demonstrate an electro-optic modulator in GaAs using a laterally doped compact photonic crystal cavity coupled to a fiber taper waveguide. The small mode volume of the cavity of $0.8(\lambda/n)^3$, over an order of magnitude smaller than typical microring resonators, along with efficient electrical injection provided by the lateral doping layout enable ultra-low power operation at potentially very high speeds.

2. Design and fabrication

The modulator design is based on a waveguide coupled to a cavity, similar to waveguide coupled SOI ring resonators. In this implementation a fiber taper serves as an adjustable waveguide and the cavity is formed out of an L3 photonic crystal defect [9]. Having a fiber taper for the waveguide allows for careful control of the loaded Q factor and transmission of the signal, as well as enables high power testing since there is minimal loss in the setup. Finite-difference time domain simulations showed that fiber taper loaded Q factors can be over 10,000 for cavities at 1500 nm and the transmission as low as 0.13 at the cavity center wavelength.

Modulator devices were formed out of a 135 nm thick gallium arsenide membrane grown on top of a 1.35 μm thick sacrificial $Al_{0.9}Ga_{0.1}As$ layer using MBE. Successive electron beam lithography steps defined the lateral implantation regions using a silicon nitride hard mask. The P region was formed by ion implantion of beryllium ions with an energy of 19 keV and a dose of $2.5x10^{15}$ cm^{-2}. The N region was formed by ion implantation of silicon ions at an energy of 71 keV and a dose of $3x10^{14}$ cm^{-2}. A 15s rapid thermal anneal at 850° C activated the beryllium to acceptor concentrations of $2\cdot10^{19}$ cm^{-3} and the silicon to donor concentrations of $2\cdot10^{18}$ cm^{-3}. To prevent arsenic outdiffusion during annealing, a thin nitride cap was used. The photonic crystal cavities were patterned with e-beam lithography and dry-etched in a BCl_3/Cl_2 chemistry. Cavities were fabricated with a lattice constant $a = 480$ nm and hole radii $r/a = 0.23$-27. Finally, a Au/Ge/Ni/Au n-type contact and a Au/Zn/Au p-type contact were deposited and the membranes were released by wet etching the sacrificial layer. For more details on the lateral PIN structure, see [10]. An SEM image of a completed cavity is shown in Fig. 1(a), where the dashed lines indicate the doping regions surrounding an intrinsic layer about 600 nm wide. The fiber taper was fabricated as in [11], and had a 1 μm waist for coupling to the PC cavities. Total fiber loss was less than 3 dB.
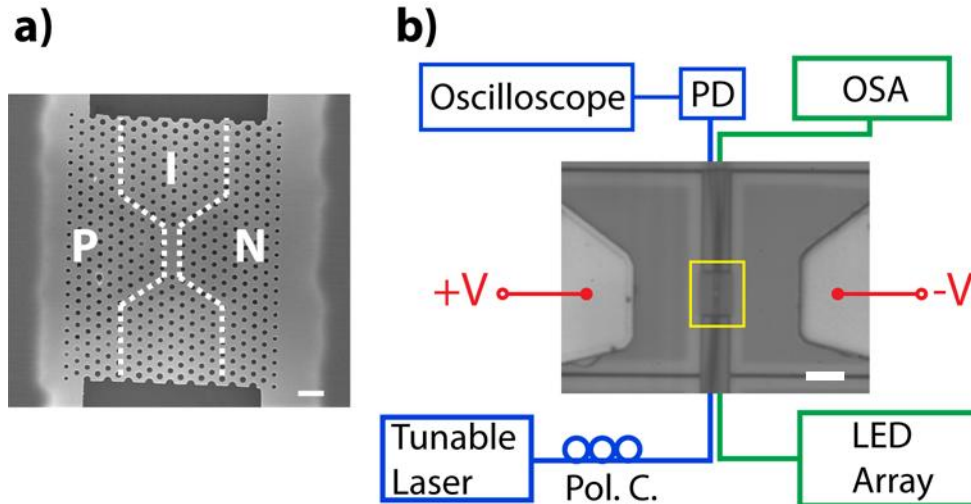
Fig. 1. (a) SEM image of a fabricated laterally doped PIN photonic crystal diode. Dashed lines indicate the approximate boundaries of the doped regions. The scale bar is 1 μm. (b) Experimental setup for probing the cavity DC transmission characteristics (green path) as well as RF modulation performance (blue path). OSA is optical spectrum analyzer, PD is photodiode, and Pol. C. is polarization controller. The cavity is outlined in the yellow box at the center of the optical picture of the setup and a fiber taper of 1 μm in diameter is seen aligned vertically. DC and RF voltages are applied to the metal contact pads to the left and right of the cavity. The scale bar is 10 μm.

3. Experiment

3.1. DC modulation

DC modulation was first performed to determine the electro-optic tuning properties of our device. The fiber taper was aligned along the long axis of the L3 cavity and positioned at a slight offset from the cavity (Fig. 1(b)), thus finding a good compromise between high Q and transmission. This ability to relocate the fiber taper to various positions allows easy optimization of the cavity coupling [12] and correspondingly modulator performance. At zero bias the Q of our cavity is 4130, lower than expected due to free carrier absorption (FCA) from the nearby doped regions. Other cavities fabricated on the same chip with no nearby doped regions had consistently higher quality factors, confirming the source of the loss. This value can be increased in the future by spacing out the doping regions by another few hundred nm.

DC electrical probes were then applied to the contacts and the cavity resonance transmission was monitored as the bias current increased. Plotted in Fig. 2(a) are several traces of the cavity transmission (using unpolarized broadband light and an optical spectrum analyzer) for 0 A, 20 nA, and 200 nA corresponding to voltages of 0, 0.67, and 1 V (inset of Fig. 2(b)). As can be seen, the cavity resonance blueshifts monotonically even for these ultra-low injection levels. In fact, 50% of the blueshift occurs in the first 20 nA of injection before saturating at approximately 200 nA (Fig. 2(b)). Beyond several μA, the cavity mode begins to redshift indicating heating caused by series resistance. The reason for the saturation behavior is because a parallel current path was discovered to exist that shunted most of the current beyond a 1 V bias. We believe this parasitic path is located in the AlGaAs layer and reaches into an unintentionally doped buffer layer that was incorporated during wafer growth. This effect can be removed with a better MBE growth method as minimal leakage current was observed for similar devices in [13]. Nonetheless, the total blueshift of 110 pm is comparable or greater than that found in most other cavity-based modulator designs [2-4] and is large enough to observe RF modulation for the present experiment. Furthermore, the value of 200

nA is over an order of magnitude lower than in previous studies [3] and promises ultra-low energy operation.
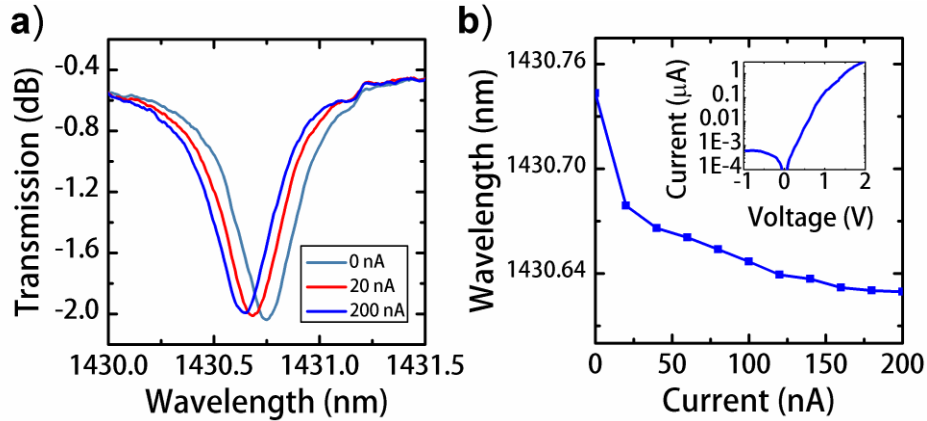

Fig. 2. (a) Optical transmission of the fiber-coupled PC cavity for several DC current magnitudes. Data is taken by sending broadband unpolarized light from an LED array and detecting the transmission with an optical spectrum analyzer. (b) Position of the cavity resonance versus injected current. The cavity blueshifts monotonically with increasing injection level reaching a 110 pm shift at 200 nA. The inset is the I-V plot of the cavity.

3.2. RF modulation

Low speed modulation was accomplished by sending a fiber-coupled tunable laser through one end of the cavity-coupled fiber taper (Fig. 1(b)). An in-line polarization controller was used to maximize the coupling to the fundamental transverse electric cavity mode and the laser wavelength was adjusted to match the steep slope of the resonance for greater contrast. A function generator signal of 2 kHz was applied to the contacts and the resultant response of a photodiode was recorded on an oscilloscope. The output modulated light for a positive swing voltage of only 1 V is seen in Fig. 3(a), with a contrast of 10%. As mentioned before, we are limited in our contrast for this particular sample due to the injection saturation caused by the parasitic current pathway; however for future devices we should be able to correct this problem.

To confirm fast switching behavior due to free carriers, we applied a 100 MHz electrical signal to our modulator and monitor the optical transmission response on a PIN photodiode with a built-in high frequency amplifier with a cutoff frequency of 1 GHz (Menlo Systems FPD 310) to better see our output. Custom high-speed probes from Cascade Microtech were used that allowed clearance between the probe tips for the fiber taper. The result in Fig. 3(b) again shows clear modulation by our device. The swing voltages for this plot are from −1.5V to 1.5V and are larger than the low frequency experiment in order to better see the signal, as the RF circuit in the detector has higher noise. Figure 3(c) shows the response at 1 GHz. Even though we are at the frequency limit of our detector equipment, we still observe modulation by our photonic crystal cavity diode. Additionally, we note that we can operate our modulator with mW laser power levels since our low Q cavity reduces two-photon absorption which causes additional FCA and cavity linewidth broadening [14].
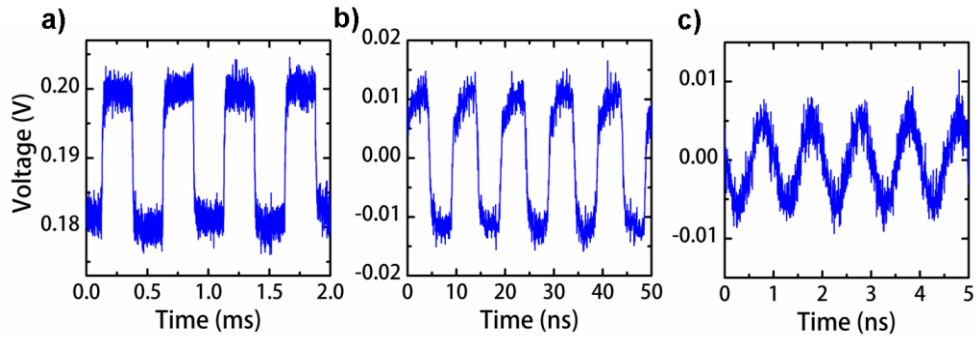
Fig. 3. (a) Operation of the modulator at 2 kHz using a 0 to 1 V square wave function. A low noise photodetector was connected to an oscilloscope for voltage visualization. (b) 100 MHz modulation from a −1.5V to 1.5V signal using a photodetector with an RF amplifier connected to the oscilloscope. (c) 1 GHz modulation with the device in the same configuration as (b). The detector is at its −3 dB point and so the signal is distorted.

3.3. Carrier lifetime

The maximum speed of our modulator is expected to be limited by the transient carrier dynamics; namely, the pull-up and pull-down speeds are roughly equivalent to the total carrier lifetime. In gallium arsenide photonic crystals, carriers recombine most rapidly due to nonradiative recombination at the etched hole surfaces [15]. To measure the total carrier lifetime we perform time-resolved photoluminescence (PL) measurements of the GaAs band-edge at room temperature. The devices are pumped by a Ti:Sapphire laser with 3 ps pulses at 80 MHz repetition rate and the PL is measured with a streak camera as in [15]. As Fig. 4 shows, the decay is very fast, corresponding to a lifetime of approximately 6 ps. This value agrees well with [15], since the decay rate has a square root dependence on temperature and the measured value in the former study at 30 K was 35 ps. Therefore, the ultimate speed of this device should be well in the tens of GHz.
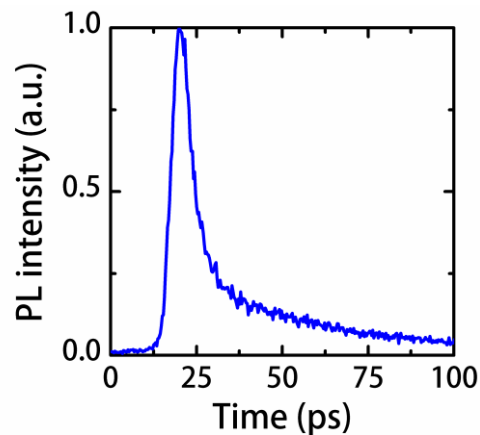

Fig. 4. Lifetime of gallium arsenide band edge PL as detected by a streak camera. The sample is pumped locally at the PC cavity defect by 3 ps Ti:Sapphire laser pulses. The decay consists of a fast component (PC cavity) and slower background component.

4. Discussion

The small mode volume of the PC cavity and the high free carrier dispersion in GaAs result in an extremely low switching energy. For an injection-based modulator, the total energy per bit

can be quantified by summing the DC energy and the transient switching energy [16]. The DC power is $P_{DC} = 0.5(IV)$, where 0.5 is used because DC current only flows half the time for a random bit sequence. From above, the current is 200 nA and the voltage is 1 V, hence the power is 100 nW. For 100 MHz modulation the energy per bit is thus $E_{DC} = 1\ fJ/bit$ and for 1 GHz modulation, $E_{DC} = 0.1\ fJ/bit$. The transient switching energy is given by the integral of the product of current and voltage over an injection cycle (weighted by 0.25 since injection occurs for one out of four bit transitions), or $E_{trans} = 0.25Q_{in}V$, where Q_{in} is the injected charge. We can approximate the injected charge by multiplying the mode volume of the cavity by the required charge density needed for a 110 pm blueshift in GaAs. For this L3 cavity the mode volume is ~0.06 μm^3 and from [6], the carrier density in GaAs corresponding to such a shift should be 4.4·10^{16} cm^{-3}. Therefore at 1 V we find $E_{trans} = 0.1\ fJ/bit$. Thus our modulator operates clearly at 1.1 fJ/bit for 100 MHz and 0.2 fJ/bit for 1 GHz.

Cavity-waveguide modulator energies are the sum total of switching energy and heater energy needed for wavelength stabilization in the case of high Q cavities [4]. Our present modulator can be modified to either work with high contrast in either a high Q or low Q configuration. For high Q operation, the doping regions should be spaced out farther to prevent free carrier absorption. The above shift of 110 pm corresponds to a linewidth of the cavity with a Q of 14,000 - the value that should be reachable on our platform. Such a device would preserve the ~0.2 fJ/bit switching energy, but requires a heater for thermal stabilization, which dissipates additional energy. On the other hand, for the low Q operation regime (such as in this article), we would need to eliminate the injection saturation caused by the current leakage path in order to shift the cavity by a full linewidth. This would increase E_{trans} by a factor of four, but could eliminate the need for the stabilizing heater (as the linewidth is much broader, and hence, the system cannot be impacted significantly by thermal instabilities).

An additional implementation of this laterally doped scheme would be a reverse-biased diode modulator. Free-carrier removal by increasing the depletion width is often a faster and lower energy process than carrier injection through forward biasing [4]. In the current experiment we have not optimized the doping concentrations and spacing between doped regions for this mode of operation, but this should be easy to design and implement. Finally, we note that all of the performance parameters could be improved in either configuration by reducing the series resistance of the diode, found here to be a few hundred kΩ, dominated by a bad contact resistance. We have observed diode series resistances as low as 1 kΩ in similar structures [13] indicating that PC holes have minimal impact on the electronic transport through membranes.

5. Conclusion

In summary, we have investigated a novel PC electro-optic modulator consisting of a GaAs cavity coupled to a fiber taper probe. The fiber taper serves as a reconfigurable waveguide that can modify the transmission and quality factor of our devices. Modulation of a probe laser beam was observed at 1 GHz with the ultimate speed of the device likely to be in the tens of GHz, due to rapid carrier recombination at PC hole surfaces. Energy calculations showed that even at 100 MHz the switching energy per bit is only ~1 fJ. We believe that simple improvements to the modulator design could allow high contrast operation at over 10 GHz speed with switching energies well below 1 fJ/bit.

Acknowledgments